

NUREG/CR-2793
SAND82-0727
R7
Printed June 1982

Techniques for Elevated Temperature Mechanical Testing

David T. Schmale, Robert W. Cross

Prepared by
Sandia National Laboratories
Albuquerque, New Mexico 87185 and Livermore, California 94550
for the United States Department of Energy
under Contract DE-AC04-76DP00789



8208260037 820821
PDR NUREG
CR-2793 R PDR

Prepared for
U. S. NUCLEAR REGULATORY COMMISSION

SF29000(8-81)

NOTICE

This report was prepared as an account of work sponsored by an agency of the United States Government. Neither the United States Government nor any agency thereof, or any of their employees, makes any warranty, expressed or implied, or assumes any legal liability or responsibility for any third party's use, or the results of such use, of any information, apparatus product or process disclosed in this report, or represents that its use by such third party would not infringe privately owned rights.

Available from
GPO Sales Program
Division of Technical Information and Document Control
U.S. Nuclear Regulatory Commission
Washington, D.C. 20555

and

National Technical Information Service
Springfield, Virginia 22161

TECHNIQUES FOR ELEVATED TEMPERATURE MECHANICAL TESTING

David T. Schmale

Robert W. Cross

Mechanical Metallurgy Division 5835

Sandia National Laboratories

Albuquerque, New Mexico 87185

ABSTRACT

Commercially available standard mechanical test systems are generally designed to do tension tests at ambient temperatures. Experimental requirements which include the sometimes mutually exclusive requirements of high temperatures, strain measurement and control, precise specimen alignment, and fully reversed loading require substantial modifications to the standard equipment. Programs in solar central receiver technology and advanced nuclear reactor safety require the examination of low cycle fatigue and creep-fatigue behaviors in several structural alloys at elevated temperatures. The specialized techniques devised to successfully perform these tests are described here along with a discussion of the differing requirements and behavior of magnetic and nonmagnetic materials.

I. INTRODUCTION

Three similar test systems are used for all testing in the high temperature mechanical properties laboratory. However, the techniques for elevated temperature mechanical testing vary with the material being tested. The temperature (up to 1300K) must remain constant and uniformly distributed within the gage length of the specimen. The specimen must be rigidly mounted to allow axial motion only. Changing stress must be applied smoothly and precisely with a concomitant accurate and sensitive method of strain measurement to provide a clean signal at low strain levels.

This report describes the equipment utilized and the techniques which are peculiar to certain alloys necessary to adapt the standard equipment to meet these requirements.

II. TEST EQUIPMENT

A. MTS* Hydraulic, Closed Loop System: Standard Components

The basic requirements of reversed loading elevated temperature fatigue testing are met with standard closed loop MTS hydraulic system components. Two-post test frames with servo-actuated, push-pull rams are used with hydraulic pressure supplied by external pumps (See Fig. 1). An MTS 442 controller with AC and DC conditioners and associated modules for servo-control monitors stroke, strain and load and provides feedback in the desired mode of operation. An MTS 410 digital function generator provides the test program for any control mode. Additional computer control and 24 hour data acquisition are possible with an MTS 433 computer interface along with a DEC PDP-11/34.

Load, stroke and strain voltages are monitored continuously with digital voltmeters during tests. Routine data acquisition is accomplished

*Complete addresses of equipment manufacturers are listed in the Appendix 1.

using x-y and strip chart recorders. A Sandia designed interlock circuit is used in addition to the MTS limit detectors to monitor temperature deviation, flow of cooling water and RF generator operation. This enables 24 hour testing while observing proper precautions in case of specimen failure or equipment malfunction.

B. Specimen & Grip Design

Specimens are button ended with a straight sided gage section machined to close tolerances. (See Appendix 2, Dwg. 1) Split collet grips are used to rigidly fix the specimen and avoid any backlash in the load train. The grip assembly provided by MTS is adequate with the exception of the split collets (Fig. 2). The collets supplied with the grips had been turned on a lathe as one piece and then cut into two collets so that the missing material from the cut result in collets that do not fit snugly around the specimen. Sandia designed replacements are machined as separate pieces to avoid this. All surfaces which are perpendicular to the load train are held to close tolerances. (See Appendix 2, Dwg. 2) The MTS supplied water-cooled fixtures do an adequate job of cooling the load train components and protecting the load cell, but the collet grips as supplied got too hot during testing, and have been modified by soldering copper water cooling tubes around their circumferences as shown also in Fig. 2. Fig. 3 shows an assembly view of a Sandia built test fixture using tapered split collet grips. The specimen is mounted in the grips first, then placed in the test frame.

The alignment of load cell and ram are checked periodically. The ram axis is used as a reference for this procedure. First, a dial indicator is used to determine the eccentricity of the lower fixture relative to the ram. This is recorded. Then the eccentricity of the upper fixture is measured, also relative to the ram. The two eccentricities are compared and

the upper is adjusted to within $\pm .001$ " of the lower by loosening and moving the load cell. Extensions with spiral washers are used to accommodate differing specimen lengths and eliminate backlash. When a specimen is mounted, it is first placed loosely in the upper grip, checked for alignment with the lower fixture (on the ram), then tightened. The RF coil is put around the specimen and temporarily held in place. The lower grip is then assembled and tightened. Since the tolerances are very close and there is only one way the assembly will fit together, alignment is ensured when the collets slide freely around the specimen within the lower fixture.

C. Temperature Control

High temperatures are attained locally within the specimen utilizing induction heating via a water cooled copper tubing coil wound around the specimen. This method is compact, allowing the grips to have the required size and rigidity for reversed load testing. A tube furnace would complicate strain measurements and load train components slender enough to fit would not have the necessary rigidity. A Lepel RF generator supplies current to the coil. A thermocouple spot welded to the specimen supplies the control signal to a Leeds and Northrup Controller Model #6432. A discussion of coil geometry and placement are included in a subsequent section of this report.

D. Strain Measurement

Strain measurements are taken directly from the gage section of the specimen with an MTS quartz rod diametral extensometer (Fig. 4) in conjunction with a DC strain conditioner. Axial extensometers, also available, provide a direct reading of axial strain, but are generally bulky and require dimpling of the specimen surface to maintain solid contact, which can

cause premature failure in fatigue tests. Diametral strain can be converted to axial strain if Poisson's ratio is known.

III. DESIGN OF HEATING COILS & PLACEMENT OF THERMOCOUPLES

A. Coil Design

Induction heating works through the generation of eddy currents in the test specimen which resistively heat it. The heating input power depends on the magnitude of the local magnetic field within the specimen. That magnitude depends on field frequency, coil geometry and the magnetic properties of the specimen. For testing ferromagnetic and non-magnetic alloys, two different coil designs are necessary: one for non-magnetic austenitic stainless steels (such as Incoloy 800, 316 and 304 stainless) and one for ferritic steels (such as 9Cr-1Mo and 2 1/4Cr-1Mo).

The coils for austenitic stainless steels are symmetrically wound with the center loop widened to allow access for the quartz rod extensometer (Fig. 5). The coils are copper tubing (1/8" dia) wound around a mandrel. It is important to note where the fittings from the RF generator and extensometer are located in the test frame so the coil can be wound to be compatible. Upon installation, using a dummy specimen instrumented with at least 3 spot welded thermocouples, the coil is bent to produce constant temperature along the entire gage section. The non-magnetic character of austenitic steels allows the coils to be fabricated and calibrated in a minimum amount of time.

Coils for the ferromagnetic steels, however, require more time and patience. These coils must be wound with the center coil opposing the others (Fig. 6). Access for the extensometer must also be provided. The reverse wound center loop is necessary because the ferromagnetism produces a strong

tendency to develop a hot spot in the gage center. The coil is then mounted in a test frame, as before with a dummy specimen, and bent until the temperature is distributed evenly. This process is sufficiently difficult and tedious that some record of final loop spacings should be made to maintain proper shape over the period of several tests. Each final coil is satisfactory only to one specimen shape; changing specimen design requires a redesigned coil. For frequently used coils it is helpful to mount them in a plexiglass holder (Fig. 6) for more permanent and precise alignment. The plexiglass holder is bolted to a three-axis translation system mounted on the load train.

B. Thermocouple Temperature Control

Placement of thermocouples for control differs between the two groups of alloys (i.e. ferromagnetic and non-magnetic). For austenitic stainless steels (Fig. 7) the control thermocouple is welded on the shoulder of the specimen with a thin wire thermocouple stretched around the gage to monitor the actual temperature there, which is usually 25-40K hotter than the shoulder. The L&N controller must be set to the shoulder temperature and adjusted to obtain the correct gage temperature. In this manner the gage temperature is held constant to within $\pm 0.5K$ without spot welding a thermocouple to the gage.

The ferromagnetism of the ferritic steels again complicates the testing procedure. A series of 9Cr-1Mo steel tests have demonstrated a temperature variation during cycling. These tests were done in load control, with the control thermocouple spot welded on the shoulder and a monitoring thermocouple on the gage. Using the type of coil shown in Fig. 6, the temperature was uniform throughout the gage to within $\pm 2K$ and remained at 866.4K (1000°F) in the center at zero load. Several reversed loading tests were run with a triangular wave form and different cycle times (t_c) between the same tensile and compressive loads well below the elastic limits in order to

characterize the resulting temperature variations. The first, $t_C = \infty$, in Fig. 8 was determined using increasing and decreasing load steps, not progressing to the next step until the temperature at the monitoring thermocouple reached equilibrium. Three consecutive cycles were then run at $t_C = 20$ minutes, 5 minutes, 2 minutes, 30 seconds and 4 seconds. Again, stress and temperature were recorded. However, only the gage section temperature is plotted against normalized time (t/t_C) in Fig. 9. As the time per cycle diminishes, the less the temperature fluctuates; until finally at $t_C = 4$ seconds it ceases to fluctuate, but decreases a small amount each cycle. Also, 70 cycles were run at $t_C = 4$ seconds to determine the stable temperature (Fig. 10). The temperature dropped more in compression than it increased in tension, hence the progression downward for smaller t_C . This has an effect on strain in the hysteresis loops recorded simultaneously with the cycling shown in Fig. 9. Fig. 11 shows that since both temperature and mechanical stress affect strain, the loops are distorted as indicated for $t_C = 20, 5$ and 2 minutes. At $t_C = 30$ seconds the effect is still noticeable (Fig. 12). At $t_C = 4$ seconds, the loop reaches an almost normal configuration after about 30 cycles, but shifts to the right $125\mu\epsilon$ because the specimen is about 10K cooler than at the start.

In order to demonstrate that this effect is mostly the result of temperature variations, equation (1) was used to determine the true mechanical axial strain from the temperature and diameter measurements:

$$\epsilon_{\text{Axial}} = \frac{1}{\nu} \left(\alpha \Delta T + \frac{d_0 - d}{d_0} \right) \quad (1)$$

where d is the specimen diameter, d_0 is the diameter at the initial temperature and no load, ΔT is the change in temperature, α is the thermal coefficient of expansion, and ν is Poisson's ratio.

A test using a similar 9Cr-1Mo specimen was performed at 700K with the load applied in steps the same as in $t_C = \infty$. This lower temperature was chosen to eliminate the creep effects present in previous tests performed at higher temperatures. Fig. 13 is a plot of stress vs. axial strain for this test. The near vertical data (*) are the uncorrected axial strains calculated from the diametral extensometer measurements and includes thermal strains. Those data and the corresponding ΔT , substituted in Equation (1), yield values of mechanical axial strain (+); the slope closely resembling the actual elastic modulus of the material at this temperature.

In order to document the fact that this stress-temperature effect does not occur in austenitic stainless steels, similar tests were performed with a specimen of alloy 800. The coil used was similar to that in Fig. 4. Temperature varied only $\pm 2K$ from 866.4K in the gage section when cycled. Simultaneously taken hysteresis loops were closed, and straight with a slope equal to the elastic modulus.

This effect is known as the magnetomechanical effect, and it requires that the control thermocouple be mounted as in Fig. 14, just below the extensometer. The result of simply moving the control thermocouple from the shoulder to center is clearly demonstrated in Figures 15, showing that with control on the gage section, temperature varies about 2K. This effectively prevents temperature variations, but spotwelding the thermocouple on the gage provides a flaw which could eventually affect the failure of the specimen. Fig. 16 depicts hysteresis loops in load control with the control thermocouple on the gage at 866K. The openness of these loops, especially at $t_C = 2$ minutes and $t_C = 30$ seconds, is thought to be due to temperature gradients within the cross sectional area of the specimen. This phenomenon

is more completely dealt with in a paper by W. B. Jones.⁽¹⁾

While the testing summarized thus far has been in load control, one 9Cr-1Mo test was performed in strain control, with a hold time of 5 minutes in tension and .06% total diametral strain (below yielding) and with the control thermocouple on the shoulder. Fig. 17 is a strip chart recording of the entire 12 cycles, temperature and load; Fig. 18 is an hysteresis loop of cycles 4 and 5, taken simultaneously with the strip chart recording. The peak temperature was 875K, as expected from the results of Fig. 9 ($t_c = 5$ minutes). Temperature dips occurred at cycling points; as the load went into compression, the specimen tried to cool rapidly but was cut short as the load returned in tension and the temperature increased again.

This result shows the complications inherent in strain controlled testing when the temperature is not constant. In this tensile hold period test, since the temperature was higher than 866.4K, the specimen diameter increased and consequently the machine applied more tension to maintain the same diameter. When the specimen reached its peak temperature, the load leveled and then relaxed a slight amount each cycle. In Fig. 17 it is evident the overall load has decreased from left to right. Such complications preclude conducting strain control tests using temperature control from a shoulder mounted thermocouple on ferromagnetic alloys.

IV. CONCLUSION

As a result of close examination, it is found that for austenitic stainless steels the best position for the control thermocouple is on the shoulder of the specimen. Ferritic steels, as the tests also indicate, require that the thermocouple be spot welded on the gage section of the specimen to avoid the large temperature variations.

Induction heating, therefore, requires that the type of alloy be considered when fabricating a coil and mounting the thermocouple on the specimen. Coil fabrication is not an exact science; a trial and error method is used. Preparation before actual testing with austenitic stainless steels takes less time and effort than for the ferritic steels, which demand a more sophisticated coil due to complicating ferrromagnetic characteristics.

In order to perform elevated temperature cyclic testing, the standard MTS systems have been modified to meet the requirements of a rigid load train, control of loads applied, cooling of load train components, and precise control of the specimen temperature. Certain compromises have been made. Proper temperature control of ferritic steels using inductive heating requires a thermocouple be spot welded on the gage, thus influencing failure. Furnace heating would be more desirable, but would complicate load train design. In addition, quartz rod extensometers must contact the specimen, complicating coil fabrication and making uniform temperature distribution within the gage more difficult.

V. RECOMMENDED DEVELOPMENTS

Several techniques could be further developed to improve capabilities and simplify the set-up procedure for elevated temperature testing. A short, compact quartz lamp radiant furnace could be used to provide uniform heating of the specimen over the gage section and eliminate the several problems inherent in inductive heating. As a more economical approach utilizing existing RF generators, a non-contacting method of strain measurement would eliminate the quartz rods, simplify coil design and allow more uniform heating of the gage section of the specimen. Optical and capacitance probe

systems are candidates for non-contact displacement measurement. An optical pyrometer used for temperature measurement and control would eliminate the need to weld a thermocouple on the gage and reduce the chances of premature specimen failure. However, the pyrometers currently available have questionable accuracies.

REFERENCES

1. W. B. Jones, "Influence of the Magnetomechanical Effect in Testing Ferritic Steel," Submitted to Scripta Metallurgica.

APPENDIX I

Equipment Manufacturers

1. MPS Systems Corporation, Box 24012, Minneapolis, Minnesota 55424
Telephone: 612-944-8000

2. Lepel High Frequency Laboratories, Inc., 59-21 Queens-Midtown Expressway,
Maspeth, NYC, NY 11378
Telephone: 212-426-4580

3. Leeds & Northrup, Executive & Administration Offices, Sunnyside Pike,
North Wales, PA 19454
Telephone: 215-643-2000

4. Three Axis Micrometer Linear Translation Stage Model #4034-M. Daedal, Inc.,
Sandy Hill Road, P.O. Box G, Harison City, PA 15636
Telephone: 412-744-4451

FIGURE CAPTIONS

- Fig. 1: Typical MTS test system. Left to right: 2 post test frame, Tektronix 4010 terminal, control electronics for hydraulics, Digital PDP11 computer.
- Fig. 2: Cutaway assembly drawing of fixtures and grips shown in Fig. 1.
- Fig. 3: Cutaway assembly drawing of fixtures and tapered split collet grips designed and built at Sandia.
- Fig. 4: MTS air cooled quartz rod extensometer used to measure diametral strain in elevated temperature testing.
- Fig. 5: RF heating coil used to heat austenitic stainless specimens.
- Fig. 6: RF heating coil used to heat ferritic steel specimen, bonded to plexiglass block for more permanent and accurate placement in test frame.
- Fig. 7: Thermocouple positioning for austenitic stainless steel specimens.
- Fig. 8: Stabilized temperature at center of specimen plotted against stress levels increased and decreased in steps; 2-4 minute intervals. The control thermocouple was on the shoulder of the specimen.
- Fig. 9: Variations in temperature at center of specimen between compressive and tensile loading within elastic limits for the first 3 cycles.
- Fig. 10: Comparison of temperature behavior at center of specimen with different control thermocouple positions. Cycle time: 4 seconds.
- Fig. 11: The effects of temperature variations on hysteresis loops for 9Cr-1Mo. (Axial load vs. diametral strain)
- Fig. 12: The effects of temperature variations on hysteresis loops for 9Cr-1Mo. (Axial load vs. diametral strain)
- Fig. 13: Stress vs. axial strain at 700K 9Cr-1Mo calculated from diametral strain readings. (+) data corrected for temperature variations.
- Fig. 14: Thermocouple position necessary for ferritic ferromagnetic steels.
- Fig. 15: Comparison of temperature behavior at center of specimen with different control thermocouple positions. Cycle time: 30 seconds.
- Fig. 16: Hysteresis loops for 9Cr-1Mo with temperature controlled at center of specimen.
- Fig. 17: Strip chart recording of load and temperature. Test run in strain control with hold time of 5 minutes in tension.
- Fig. 18: Hysteresis loop for 9Cr-1Mo specimen; axial load vs. diametral strain.

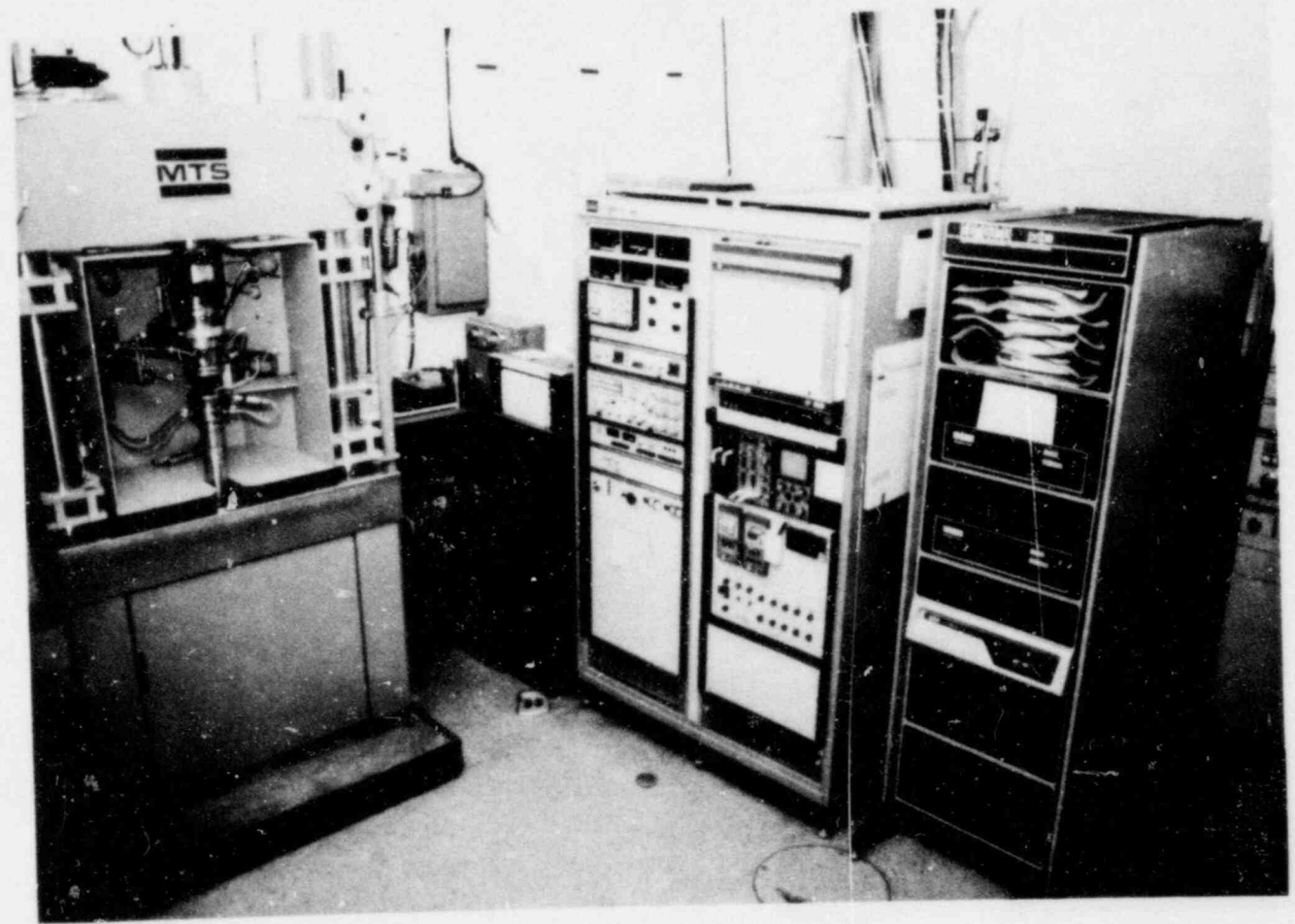


FIG. 1 Typical MTS test system. Left to right: 2 post test frame, Tektronix 4010 terminal, control electronics for hydraulics, Digital PDP11 computer.

MODIFIED MTS TEST FIXTURE ASS'Y

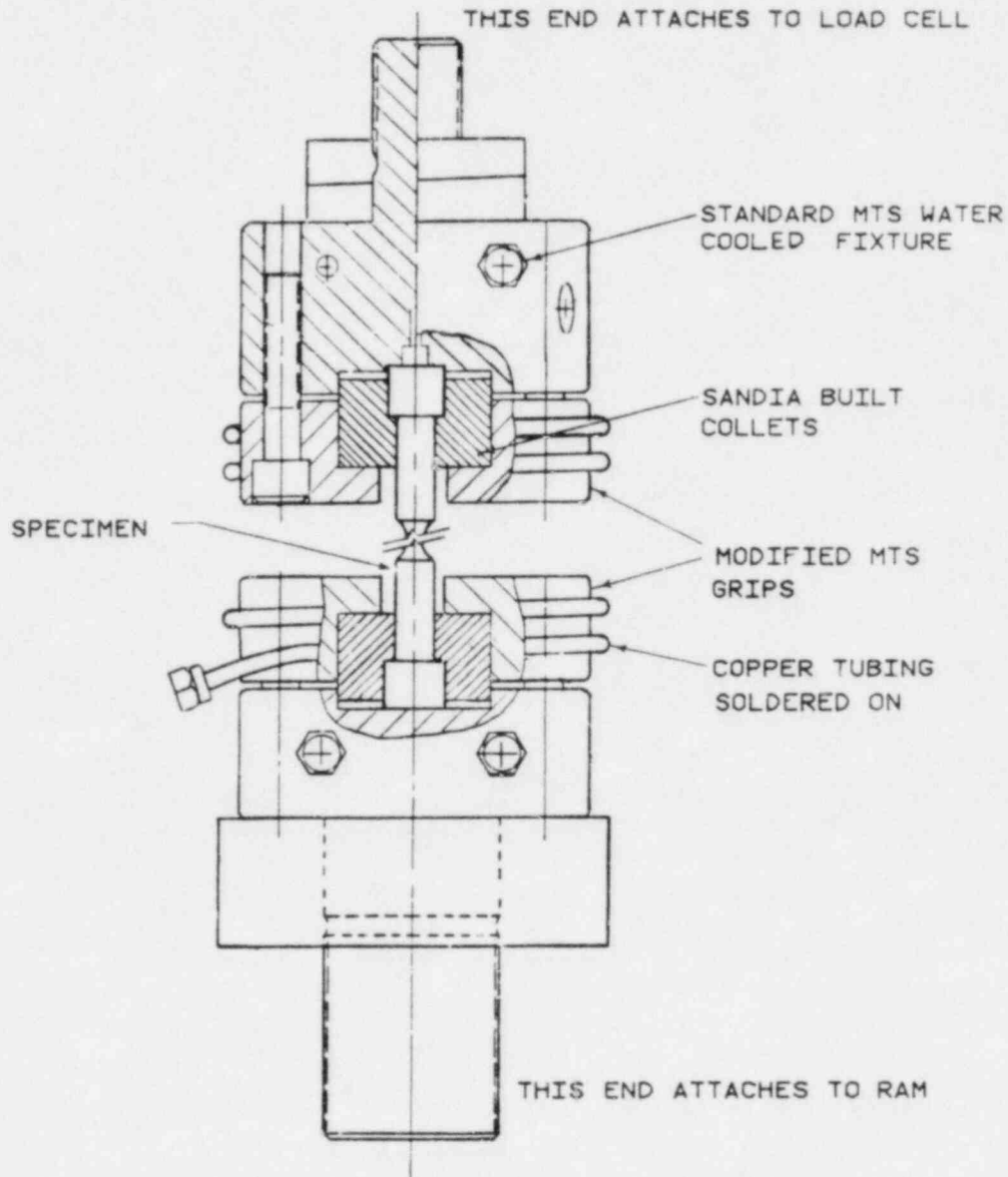


FIG. 2 Cutaway assembly drawing of fixtures and grips shown in Fig. 1.

SANDIA BUILT TEST FIXTURE ASS'Y

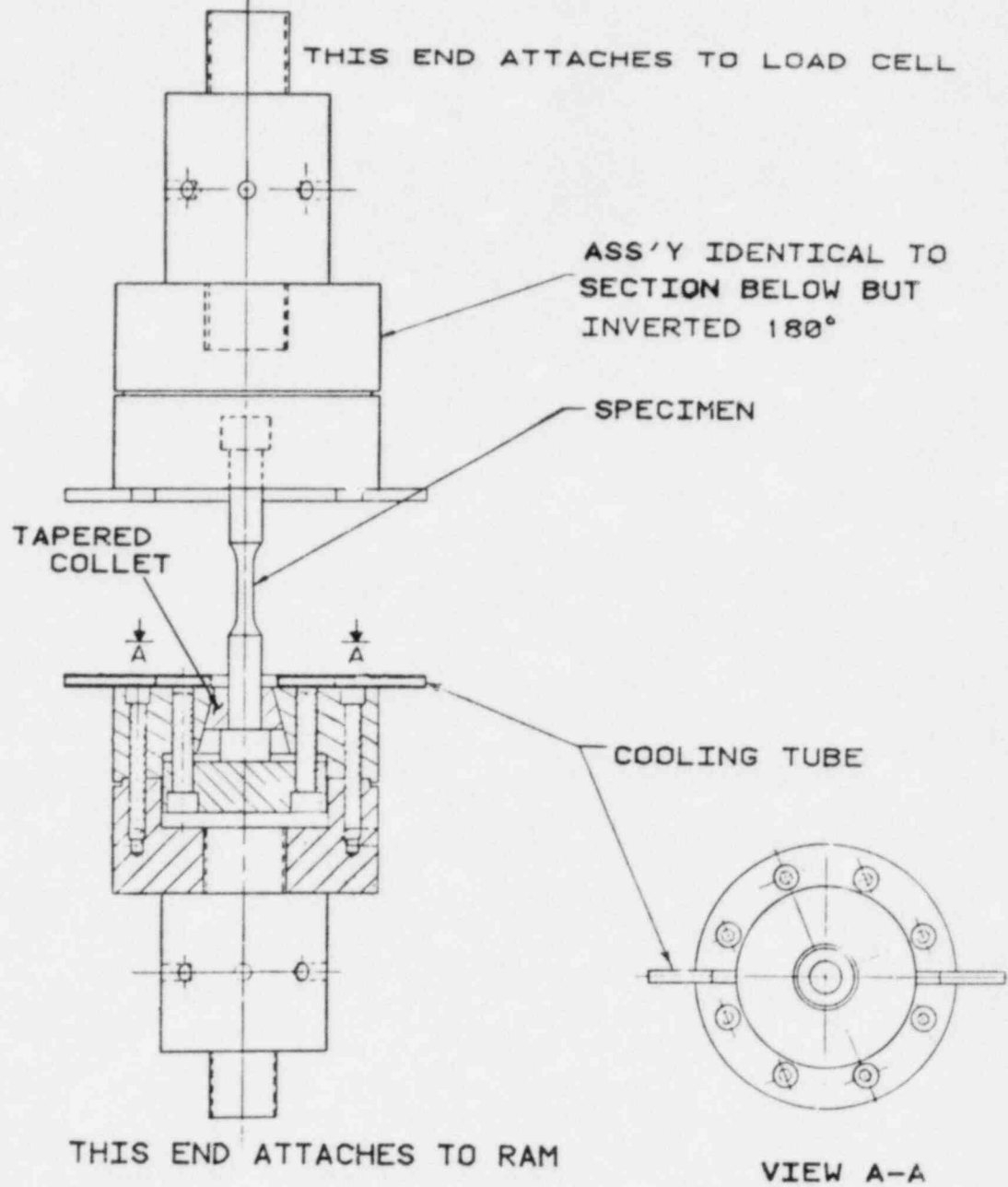


FIG. 3 Cutaway assembly drawing of fixtures and tapered split collet grips designed and built at Sandia.

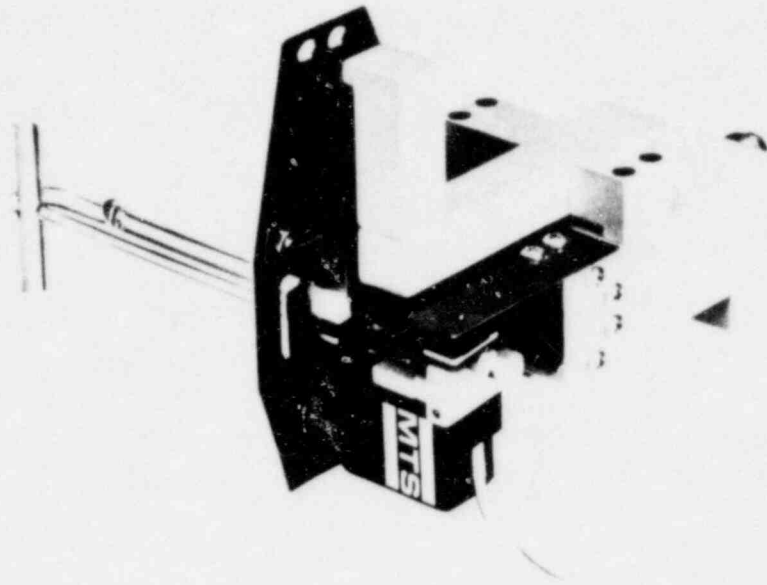


FIG. 4 MTS air cooled quartz rod extensometer used to measure diametral strain in elevated temperature testing.

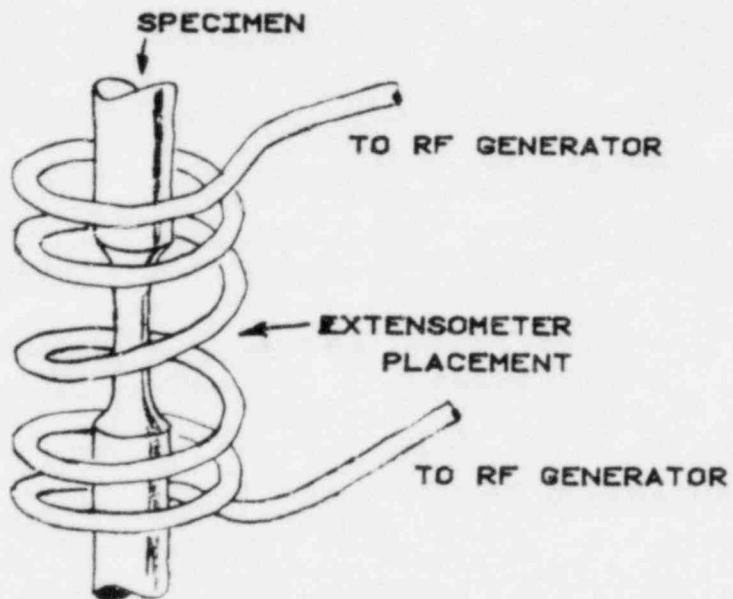


FIG. 5 RF heating coil used to heat austenitic stainless specimens.

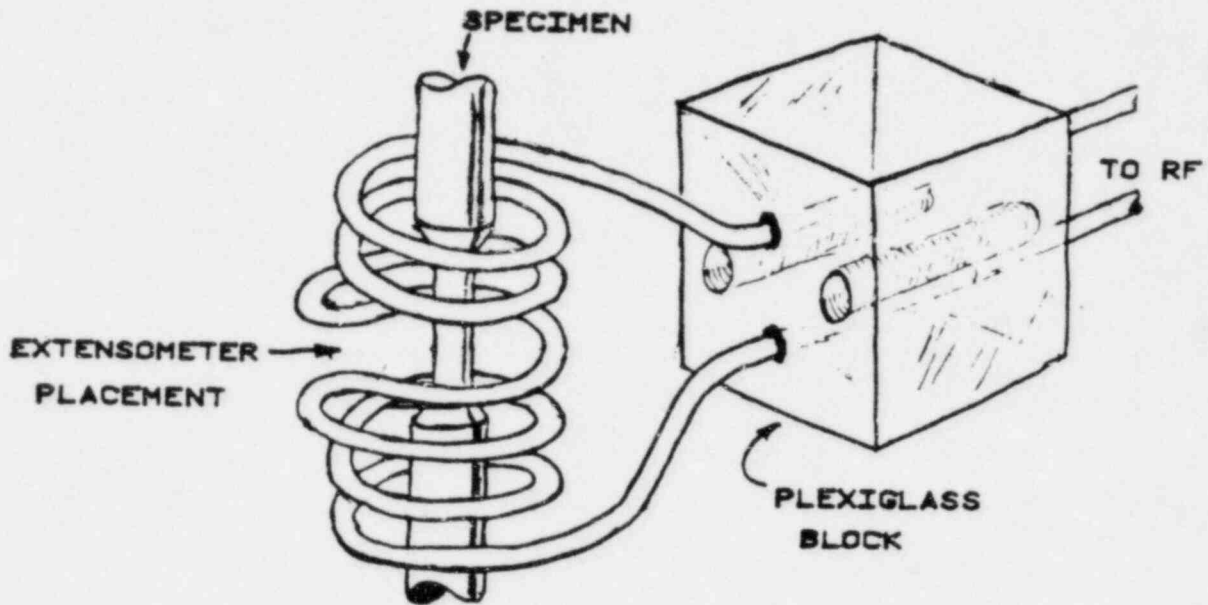


FIG. 6 RF heating coil used to heat ferritic steel specimen, bonded to plexiglass block for more permanent and accurate placement in test frame.

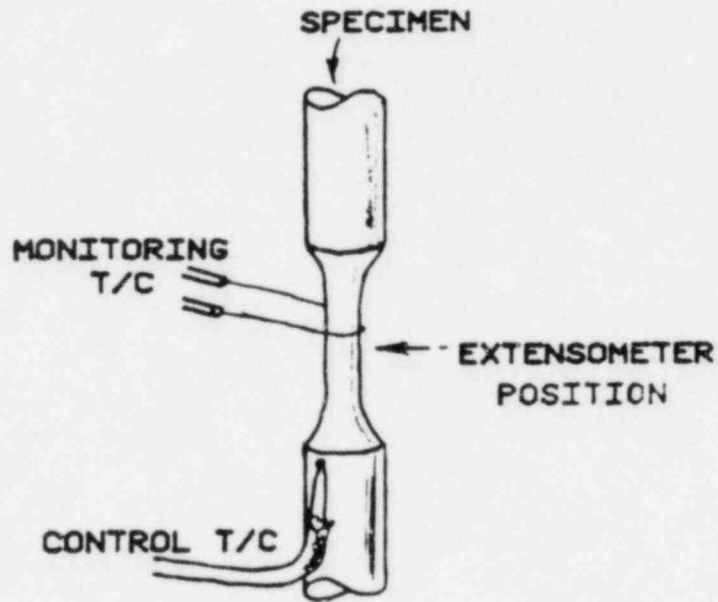


FIG. 7 Thermocouple positioning for austenitic stainless steel specimens.

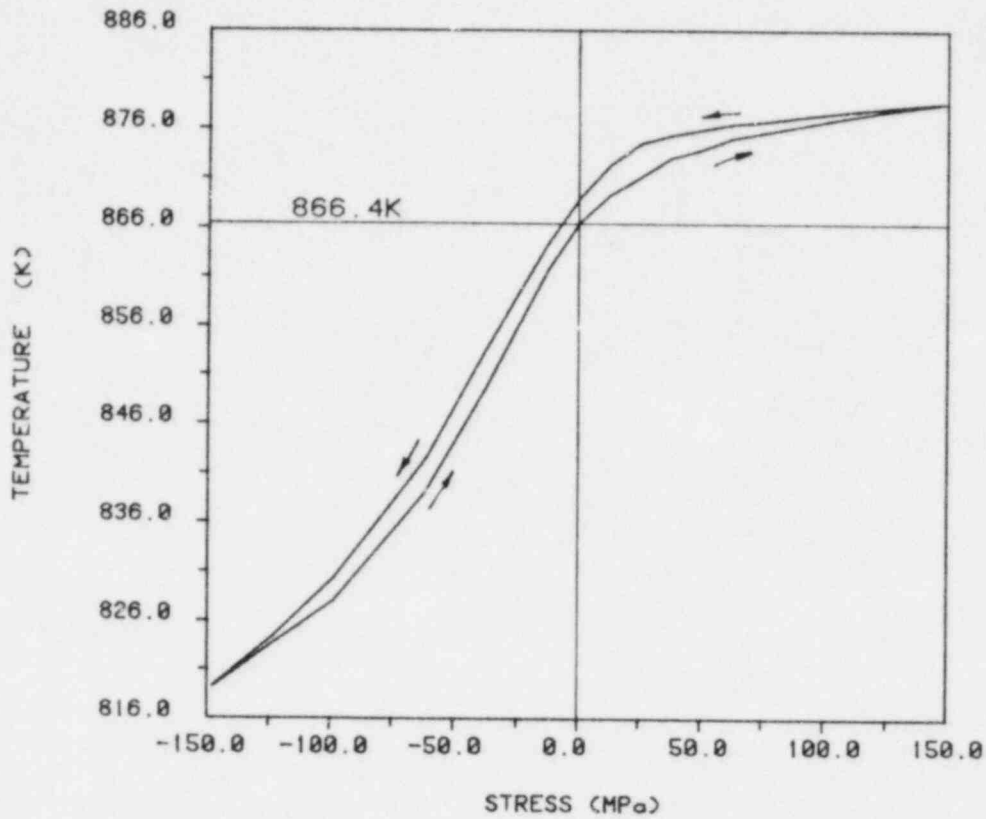


FIG. 8 Stabilized temperature at center of specimen plotted against stress levels increased and decreased in steps; 2-4 minute intervals. The control thermocouple was on the shoulder of the specimen.

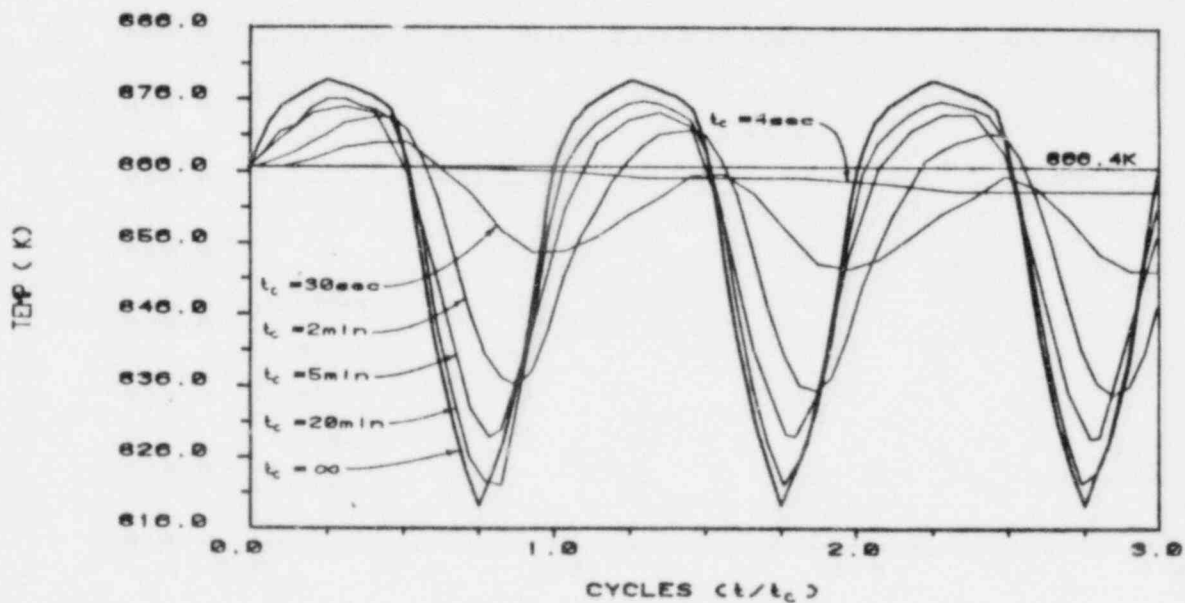


FIG. 9 Variations in temperature at center of specimen between compressive and tensile loading within elastic limits for the first 3 cycles.

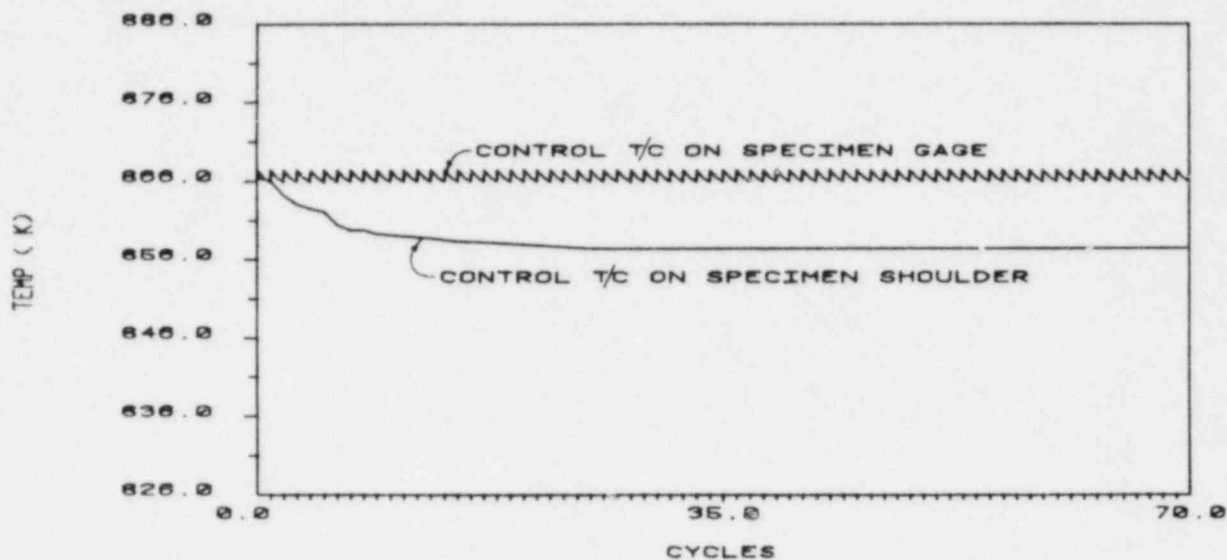


FIG. 10 Comparison of temperature behavior at center of specimen with different control thermocouple positions. Cycle time: 4 seconds.

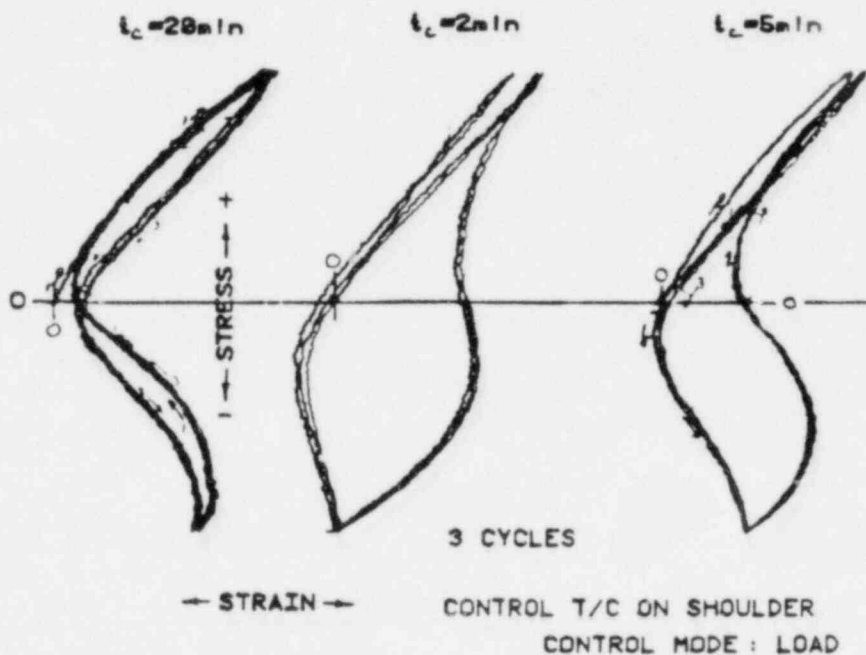


FIG. 11 The effects of temperature variations on hysteresis loops for 9Cr-1Mo. (Axial load vs. diametral strain).

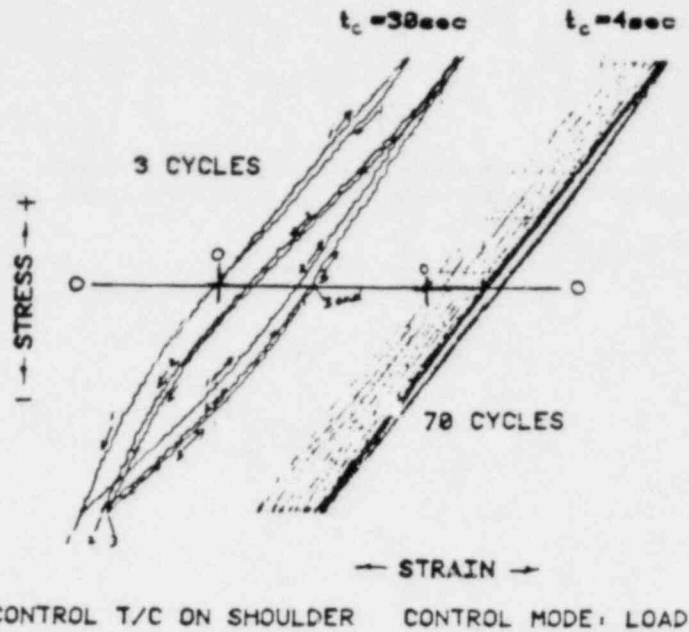


FIG. 12 The effects of temperature variations on hysteresis loops for 9Cr-1Mo. (Axial load vs. diametral strain).

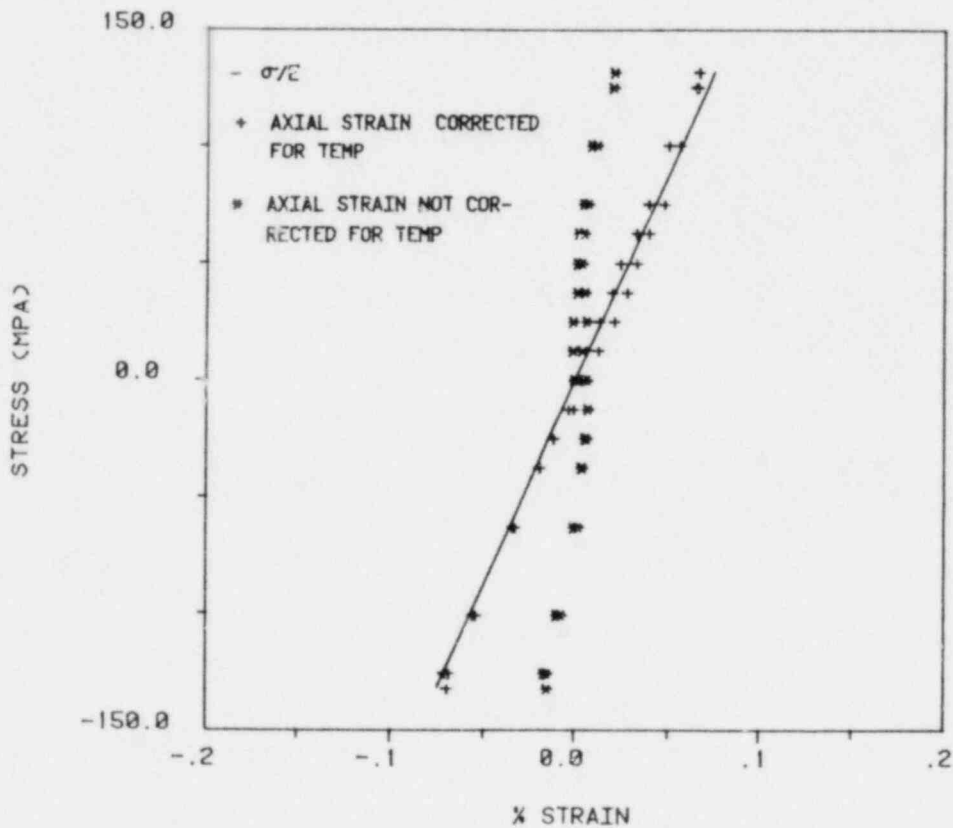


FIG. 13 Stress vs. axial strain at 700K 9Cr-1Mo calculated from diametral strain readings. (+) data corrected for temperature variations.

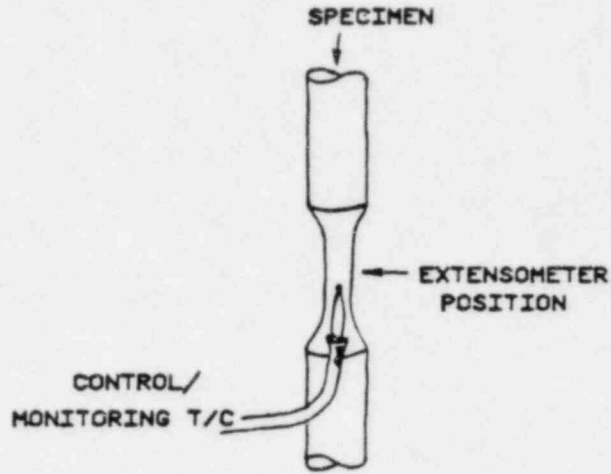


FIG. 14 Thermocouple position necessary for ferritic ferromagnetic steels.

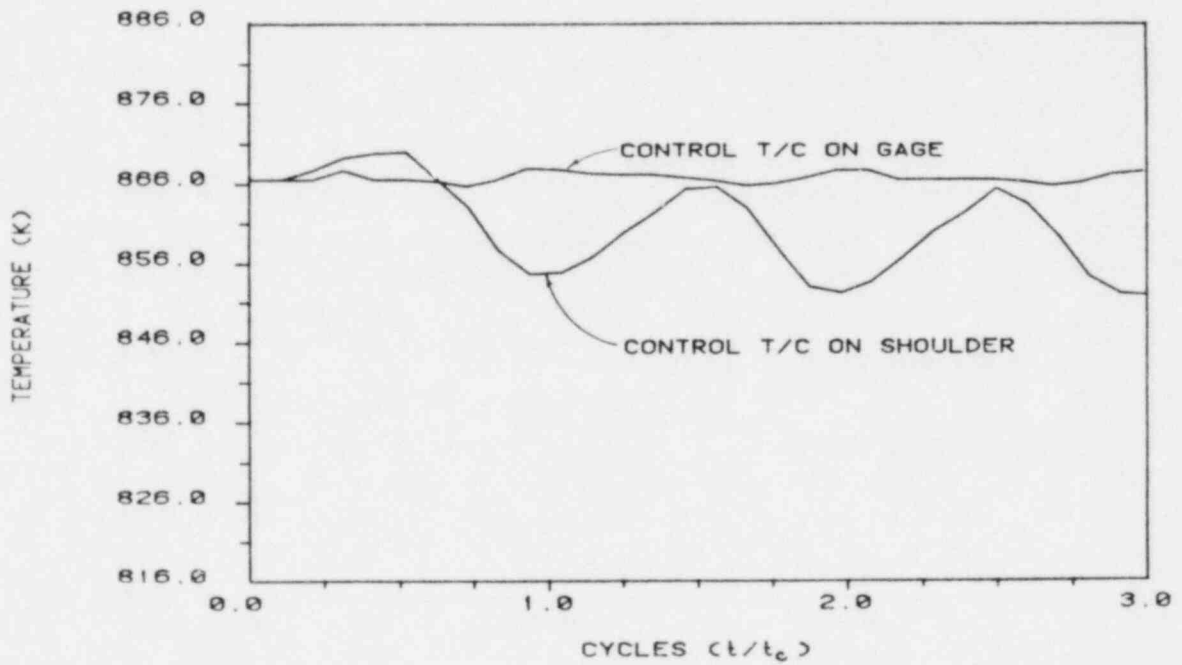


FIG. 15 Comparison of temperature behavior at center of specimen with different control thermocouple positions. Cycle time: 30 seconds.

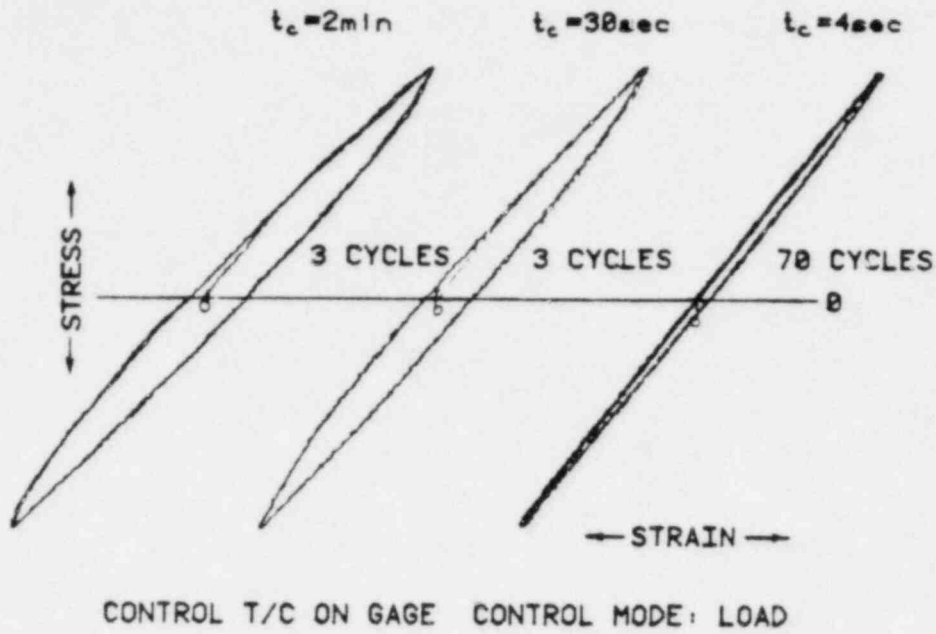


FIG. 16 Hysteresis loops for 9Cr-1Mo with temperature controlled at center of specimen.

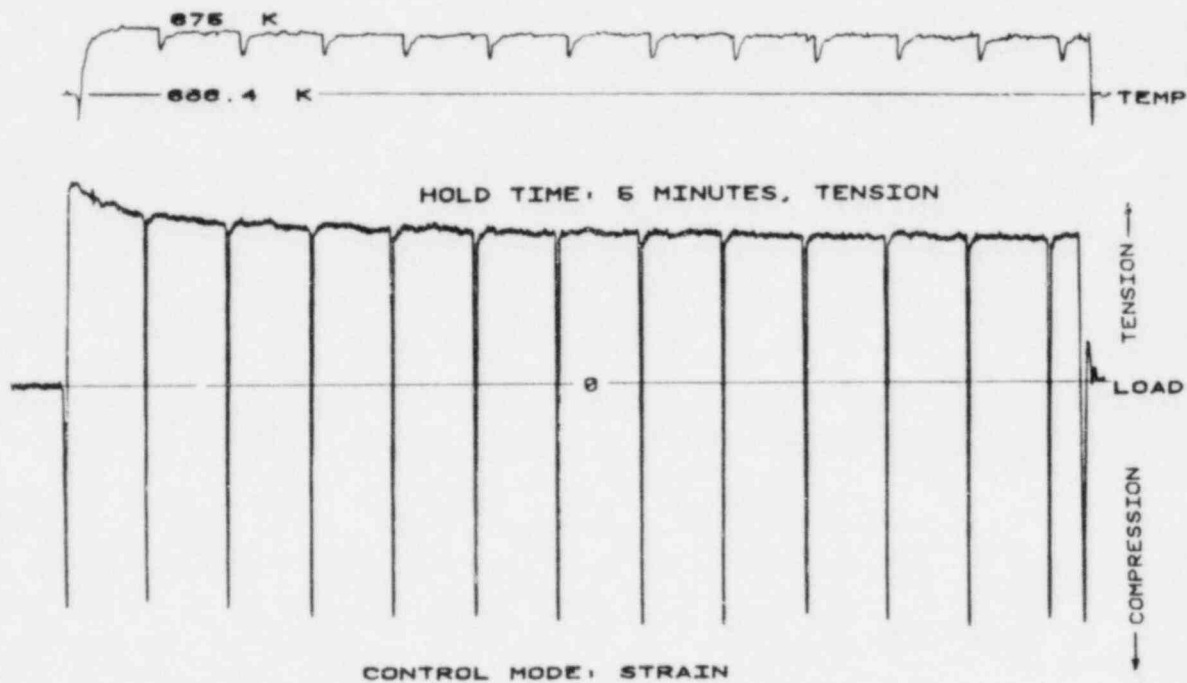
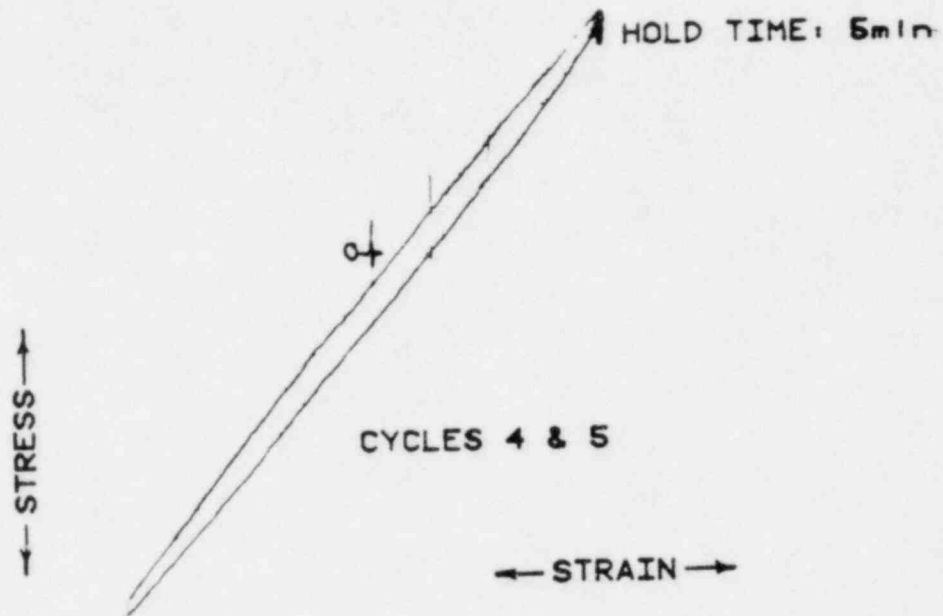


FIG. 17 Strip chart recording of load and temperature. Test run in strain control with hold time of 5 minutes in tension.

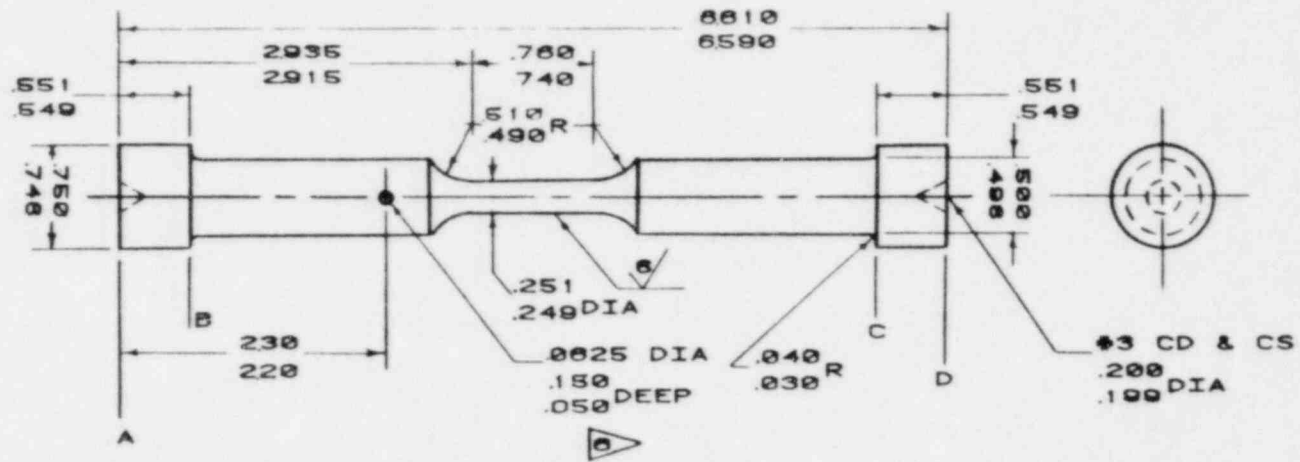


CONTROL T/C ON SHOULDER CONTROL MODE: STRAIN

FIG. 18 Hysteresis loop for 9Cr-1Mo specimen; axial load vs. diametral strain.

Drawing 2

APPENDIX II




NOTES:

1. SURFACES A, B, C AND D TO BE // WITHIN ± 0.001
2. SURFACES A, B, C AND D TO BE \perp TO AXIAL CL WITHIN ± 0.0005
3. RADIUS AND REDUCED SECTION TO BLEND SMOOTHLY WITHOUT UNDERCUT.
4. ALL DIA'S TO BE CONCENTRIC WITHIN ± 0.001
5. RADIUS & REDUCED SECTION TO BE FINISHED USING LOW STRESS GRINDING, AND FINAL FINISH OBTAINED WITH LAPPING OPERATION IN THE AXIAL DIRECTION.

 ORIENT HOLE TO INDICATE PLATE SURFACE (SEE DWG JHB200).

DIMENSIONS IN INCHES

SURFACES  EXCEPT WHERE SPEC'D

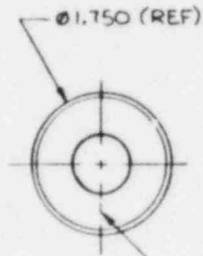
LOW CYCLE FATIGUE
ORIENTED SPECIMEN

MTI-1040A

MATL-SUPPLIED-

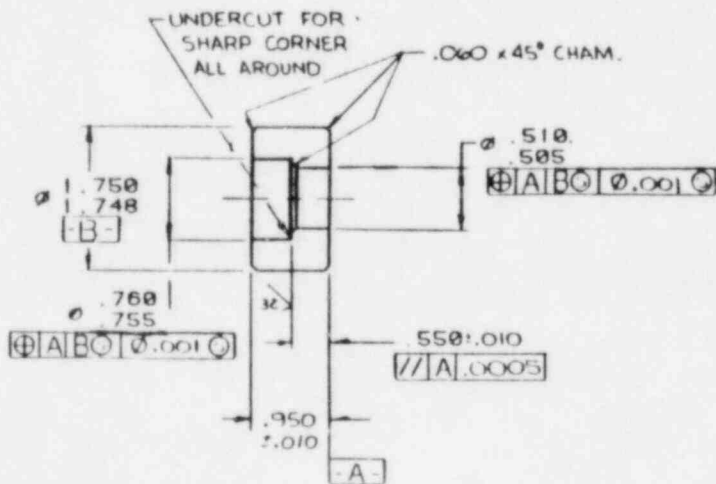
NOTES

1. FOR GENERAL REQUIREMENTS SEE 9900000.
2. MATERIAL: STAINLESS STEEL, 15-5PH VAR.
3. ϕ FINISH UNLESS OTHERWISE SPECIFIED.
4. HEAT TREAT TO RC 38-42.



\square .0005

FABRICATE COLLET BY CLAMPING TWO PIECES OF MATERIAL TOGETHER AND MACHINE TO THE SPECIFIED DIMENSIONS.



COLLET, SPECIMEN UNIAXIAL	
DWG NUMBER	T58751A

Distribution:

U. S. Nuclear Regulatory Commission
(380 copies for R7)
Division of Document Control
Distribution Services Branch
7920 Norfolk Avenue
Bethesda, MD 20014

U. S. Nuclear Regulatory Commission (54)
Division of Reactor Safety Research
Office of Nuclear Regulatory Research
Washington, DC 20555
Attn: C. N. Kelber, Assistant Director,
Advanced Reactor Safety Research
R. T. Curtis, Chief
Analytical Advanced Reactor Safety
Research, ARSR
T. J. Walker (50)
M. Silberberg, Chief
Experimental Fast Reactor Safety

U. S. Department of Energy
Office of Nuclear Safety Coordination
Washington, DC 20545
Attn: R. W. Barber

U. S. Department of Energy (2)
Albuquerque Operations Office
P. O. Box 5400
Albuquerque, NM 87185
Attn: J. R. Roeder, Director
Operational Safety Division
D. K. Nowlin, Director
Special Programs Division
For: C. B. Quinn
D. Plymale

B. C. Wei
Division of Reactor Development
and Demonstration
Department of Energy
Mail Stop F-309
Washington, DC 20545

C. R. Brinkman (4)
Metals and Ceramics Division
Oak Ridge National Laboratory
P. O. Box X
Oak Ridge, TN 37830
Attn: V. K. Sikka
J. P. Strizak
M. K. Booker

Reactor Division (4)
Oak Ridge National Laboratory
P. O. Box "Y"
Oak Ridge, TN 37830
Attn: J. M. Corum
C. E. Pugh
R. Huddleston

General Atomic Company (2)
P. O. Box 81608
San Diego, CA 92138
Attn: D. I. Roberts
J. L. Kaae

Rockwell International (2)
Atomics International Division
8900 De Soto Avenue
Canoga Park, CA 91304
Attn: H. M. Minami
R. I. Jetter

Harry Kraus
Rensselaer Polytechnic Institute
of Connecticut
275 Windsor Street
Hartford, CT 06120

E. Krempl
Dept. of Mechanical Engineering
Rensselaer Polytechnic Institute
Troy, NY 12181

M. Lemcoe
Battelle Memorial Institute
505 King Avenue
Columbus, OH 43201

M. J. Manjoine
Westinghouse Electric Corp.
Research & Development Center
1310 Beulah Road
Pittsburgh, PA 15235

S. S. Manson
Dept. of Mechanical Engineering
Case Western Reserve University
Cleveland, OH 44106

G. Halford
Mail Stop 49-1
NASA-Lewis Research Center
21000 Brook Park Road
Cleveland, OH 44135

I. Berman
Foster Wheeler Corporation
12 Peachtree Hill Road
Livingston, NJ 07039

Foster Wheeler Corporation (2)
110 South Orange Avenue
Livingston, NJ 07039
Attn: D. H. Pai
J. M. Chern

General Electric Company (2)
175 Curtner Avenue
San Jose, CA 95125
Attn: J. F. Copeland, M/C 513
C. Schmidt MIC 513

J. B. Conway
Mar-Test Incorporated
45 Novner Drive
Cincinnati, OH 45215

A. W. Dalcher
Advanced Technology Department
General Electric Company
310 Dequigne Drive
Sunnyvale, CA 94086

Argonne National Laboratory (4)
9700 South Cass Avenue
Argonne, IL 60439
Attn: A. P. L. Turner
S. Majumdar

C. H. Wells
Southwest Research Institute
8500 Culebra Road
San Antonio, TX 78228

S. Zamrick
Engineering Mechanics
Pennsylvania State University
105 Hammond Building
University Park, PA 16802

C. Chan
Nuclear Safety and Analysis Prog.
Electric Power Research Institute
P. O. Box 10412
Palo Alto, CA 94304

M. Reich
Brookhaven National Laboratory
Upton, NY 11973

C. C. Schultz
The Babcock & Development Center
P. O. Box 835
Alliance, OH 44601

Hanford Engineering and Development
Laboratory (2)
P. O. Box 1970
Richland, WA 99252
Attn: M. J. Anderson
L. K. Severud

Combustion Engr., Inc. (2)
1000 Prospect Hill Road
Windsor, CT 06095
Attn: R. Barsoum
C. W. Lawton

D. M. Norris
Lawrence Livermore Laboratory
P. O. Box 808
Livermore, CA 94550

W. J. O'Donnell
O'Donnell & Associates, Inc.
5100 Centre Avenue
Pittsburgh, PA 15232

Westinghouse Electric Corp. (2)
Advanced Reactors Division
P. O. Box 158
Madison, PA 15663
Attn: D. S. Griffin
A. L. Snow

J. Hagstrom
Chicago Bridge & Iron Co.
800 Jorie Boulevard
Oak Brook, IL 60521

1100 C. D. Broyles
Attn: J. D. Kennedy, 1110
T. L. Pace, 1120
G. L. Ogle, 1125

1537 N. R. Keltner
1537 R. U. Acton
1537 T. Y. Chu
2150 C. B. McCampbell
3141 L. J. Erickson (5)
3151 W. L. Garner (3)
3154-3 C. Dalin (25)
For: NRC Distribution to NTIS

3434 B. N. Yates
4000 A. Narath
4231 J. H. Renken
4400 A. W. Snyder
4410 D. J. McCloskey
4420 J. V. Walker (5)
4421 R. L. Coats
4421 J. E. Gronager
4421 J. T. Hitchcock
4421 G. W. Mitchell
4421 C. Ottinger
4421 J. B. Rivard
4422 D. A. Powers
4422 R. M. Elrick
4422 J. E. Smaardyk
4422 D. W. Varela
4423 P. S. Pickard
4423 A. C. Marshall
4423 D. A. McArthur
4423 K. O. Reil
4424 M. J. Clauser
4424 E. R. Copus
4424 E. F. Haskin
4424 P. J. McDaniel
4424 J. P. Odom
4424 F. W. Sciacca
4424 M. E. Senglaub
4424 D. C. Williams
4425 W. J. Camp
4425 E. Bergeron
4425 W. M. Breitung
4425 F. Briscoe
4425 R. J. Lipinski
4425 K. K. Murata
4425 M. L. Schwarz

4425 A. Soo-Anttila
4425 M. F. Young
4426 G. L. Cano
4426 J. G. Kelly
4426 H. L. Scott
4426 K. T. Stalker
4426 W. H. Sullivan
4426 S. A. Wright
4441 M. L. Corradini
4450 J. A. Reuscher
4451 T. R. Schmidt
4452 M. Aker
4723 D. O. Lee
5500 O. E. Jones
5530 W. Herrmann
5534 D. A. Benson
5541 W. Luth
5800 R. S. Claassen
5820 R. E. Whan
5822 K. H. Eckelmeyer
5830 M. J. Davis
5832 R. W. Rohde
5833 J. L. Jellison
5834 D. M. Mattox
5835 D. T. Schmale (4)
5835 R. W. Cross (4)
5836 J. L. Ledman
5837 R. S. Blewer
5846 E. K. Beauchamp
8123 W. D. Zinke
8214 M. A. Pound
8310 D. M. Schuster
8314 A. J. West
8316 J. C. Swearigen

